

RESEARCH ARTICLE

OPEN ACCESS

## ***Fusarium* Induced Anatomical and Biochemical Alterations in Wild Type and DPA-treated Wheat Seedlings**

Abhaya Kumar Sahu<sup>1</sup> , Punam Kumari<sup>1\*</sup>  and Bhabatosh Mittra<sup>1,2</sup>

<sup>1</sup>P.G.Department of Biosciences and Biotechnology, Fakir Mohan University, Vyasa Vihar, Balasore - 756089, Odisha, India.

<sup>2</sup>MITS School of Biotechnology, Bhubaneswar - 751024, Odisha, India.

### **Abstract**

Wheat (*Triticum aestivum*) employs various strategies to defend against *Fusarium oxysporum*, a soil-borne vascular fungal pathogen that disrupts structural integrity and metabolism. The purpose of this research was to ascertain the alterations of anatomical and biochemical responses in wild-type (WT) and DPA-treated wheat (*T. aestivum*) seedlings exposed to *F. oxysporum*. The WT and DPA-treated seedlings showed disorganization of parenchyma cells, sclerenchyma cells, vascular bundles (VBs), and lower numbers of xylem (Xy) and phloem (Ph) cells, and reduced thickness of the cuticle layer (C) at the epidermal layer of shoots. The content of chlorophyll (Chl), carbohydrate, and nucleic acid was reduced in WT and DPA-treated seedlings during infection. Enhanced defense responses through peroxidase (POD), and polyphenol oxidase (PPO) was observed to be high in WT as compared to DPA-treated seedlings under stress condition. In addition, the content of salicylic acid (SA) and phenolics was increased in WT than DPA under stress condition. However, the DPA-treated seedlings showed enhanced growth of fungal mycelia compared to WT during stress condition. Hence, the anatomical and biochemical aspects of DPA-treated seedlings decreased as compared to WT when exposed to *F. oxysporum*.

**Keywords:** *Triticum aestivum*, *Fusarium oxysporum*, Anatomy, PPO, SA, Phenolics

\*Correspondence: punam.lifescience@gmail.com

**Citation:** Sahu AK, Kumari P, Mittra B. *Fusarium* Induced Anatomical and Biochemical Alterations in Wild Type and DPA-treated Wheat Seedlings. J Pure Appl Microbiol. 2024;18(1):229-242. doi: 10.22207/JPAM.18.1.06

© The Author(s) 2024. **Open Access.** This article is distributed under the terms of the [Creative Commons Attribution 4.0 International License](https://creativecommons.org/licenses/by/4.0/) which permits unrestricted use, sharing, distribution, and reproduction in any medium, provided you give appropriate credit to the original author(s) and the source, provide a link to the Creative Commons license, and indicate if changes were made.

## INTRODUCTION

Plant growth and productivity are detrimentally impacted by nature's fury in the form of ecological stress components. Approximately, 96.5% of rural land areas is influenced by biotic stressors in worldwide and damaged 70% of crops.<sup>1</sup> Wheat (*Triticum aestivum*) is one of the world's most significant staple food crops due to its high nutritional value but often suffers from *Fusarium oxysporum* infection in many regions (Australia, China, Indonesia, Malaysia, Philippines, and India). Numerous species of *Fusarium*, such as *F. oxysporum*, *F. tabacinum*, *F. solani*, *F. sulphureum*, *F. avenaceum*, and *F. eumartii* are wheat-specific and responsible for *Fusarium* wilts.<sup>2</sup> Wheat has played an outstanding role in feeding a hungry world and the demand for wheat is rising worldwide due to the increasing rate of human population.<sup>3</sup>

*F. oxysporum* is a soil-borne vascular pathogen promotes wilt disease in plants. The spores of *F. oxysporum* can penetrate into the cracks or wounds at the root region.<sup>4</sup> Inside the root, the parenchymatous tissues are occupied by young mycelia, which invade the endodermis as well as reach at the xylem (Xy) vessels via pits. The Xy vessels are blocked due to microconidial spore, consequently lowering the transpiration rate, which causes profound cytological changes resulting in wilt symptoms.<sup>5</sup> The surrounding parenchyma and sclerenchyma cells changed their structure to defend the *Fusarium* proliferation and crushed the vessels in the vascular system. This induces wilting of the whole plant, which ultimately results in death.<sup>6</sup> In addition, the palisade parenchyma cells were observed to be smaller, and thinner leaf blades in plants during infection. It reduces photosynthesis and transpiration in leaves, and it inhibits the growth of roots and shoots.<sup>7</sup> A thick layer of cuticle was appeared at the upper epidermis in infected plants as compared with healthy plants.<sup>8</sup> Garcia-Viera et al.<sup>9</sup> reported that papaya ring spot virus caused histochemical changes include distorted palisade cells and disintegrated spongy cells in the leaves of papaya plants. The persistent of disease symptoms are characterized by foliar chlorosis followed by folding and stunting of plants.

*Fusarium* causes significant damage to crucial biological components such as lipids, proteins, DNA, and RNA,<sup>10</sup> stimulates the abundance of reactive oxygen species (ROS), inhibits growth, and development with tissue necrosis.<sup>6</sup> To neutralize the ROS-induced oxidative stress inside VBs, the plants have developed a basal defense system by the induction of salicylic acid (SA), which promotes the synthesis of phenolics that organize the secondary cell wall of internal tissue during infection,<sup>11</sup> and also antioxidant system, i.e., enzymatic [ascorbate peroxidase (APX), polyphenol oxidase (PPO), catalase (CAT), peroxidase (POD), superoxide dismutase (SOD), and non-enzymatic glutathione (GSH), and ascorbate (ASC)].<sup>12</sup> In addition, the phenol synthesizing PAL enzyme was inhibited by 2,4-DPA, which significantly reduce the level of intermediates of the phenylpropanoid pathway in *Lycopersicon esculentum*.<sup>13</sup> It is also reported that suppression of phenolics content induced susceptibility against fungal pathogens in wheat, tobacco, and flax plants.<sup>14</sup>

It is well established that *Fusarium* induced wilt disease impaired the anatomical and biochemical level of wheat seedlings due to disintegrated vascular bundles (VBs), reduced photosynthetic activity, SA, and phenolic contents.<sup>15</sup> Therefore, the goal of the current study was to identify the anatomical and biochemical alterations in wheat seedlings after *Fusarium* invasion.

## MATERIALS AND METHODS

### Plant material and growth condition

Wheat seeds (*T. aestivum*) were surface sterilized using 0.01% HgCl<sub>2</sub>, followed by three times washing with sterile distilled water. In order to promote germination, the sterilized seeds were incubated in sterilized petri dishes lined with wet muslin cloth for 4-5 d at room temperature (RT). Sprouted seeds were kept in a growth chamber for 7 d at 32°C, 80% relative humidity (RH), with 16 h photoperiod (240 µmol/ m<sup>2</sup>s) and an 8 h dark period at 26°C, 70% RH.<sup>16</sup> Young wheat seedlings were transported to sterilized glass test tubes containing distilled water after 7 d. One set of seedlings was cultured with 1 ml of 1 mM 2,4-DPA

suspension for 48 h at room temperature.<sup>17</sup> In the control set, seedlings were grown in distilled water and kept under non-stressed condition.

### Pathogen inoculation

*F. oxysporum* was propagated in dim light at  $28 \pm 2^\circ\text{C}$  for 4 d to produce efficient sporulation. After that, the wheat seedlings were inoculated with 4 d old *F. oxysporum* spores ( $1 \times 10^6$  spores  $\text{ml}^{-1}$ ) by pouring the spore culture into each set of test tubes and keeping them for another 7 d for further growth and development under stressed condition.

### Localization of fungal structure

The fungal structures present inside the shoot tissues were observed under light microscope after decolorized with acetic acid: ethanol: water (2:2:1) solution at room temperature and stained with lactophenol cotton blue by protocol of Charya and Garg.<sup>18</sup>

### Anatomical studies

The decolorized shoot sections were stained with toluidine blue for viewing anatomical structures using a light microscope.<sup>19</sup>

### Assay of photosynthetic pigments and CSI

The ice-chilled 80% acetone was used for homogenization of fresh shoot tissue (0.5 g) and centrifuged at 4500 rpm for 10 min at  $4^\circ\text{C}$ . The absorbance of the supernatant was read at 663, 645, and 665 nm.<sup>20</sup>

The chlorophyll content was estimated by utilizing the following formula:

$$\text{Chl a (mg/mL)} = -1.93A_{646} + 11.93A_{663}$$

$$\text{Chl b (mg/mL)} = 20.36A_{646} - 5.50A_{663}$$

$$\text{Chlorophyll a+b (Chl) (mg/mL)} = 6.43A_{663} + 18.43A_{646}$$

According to Sairam et al.,<sup>21</sup> the CSI was estimated and calculated as follows:

$$\text{CSI} = (\text{Total chlorophyll under stress} / \text{Total chlorophyll under control}) \times 100$$

### Assay of $\text{O}_2^{\bullet-}$

The localization of  $\text{O}_2^{\bullet-}$  was carried out histochemically in shoot samples using the protocol outlined by Pyngrope et al.<sup>22</sup> The shoot tissue samples were dipped in a sterilized glass beaker containing 6 mM Nitro Blue Tetrazolium

Chloride (NBT) and 10 mM sodium azide solution ( $1 \text{ mg mL}^{-1}$ , pH-7.5) for 12 h in the dark at RT. The leaf samples were again dipped in decolorizer reagent and boiled for 5 min to decolorize them. After the decolorization, the localized  $\text{O}_2^{\bullet-}$  was visualized as purple spots. In addition, the  $\text{O}_2^{\bullet-}$  content was also calculated using the protocol of Pyngrope et al.<sup>22</sup> The shoot tissues were dipped in 3 ml of a 10 mM  $\text{K}_3\text{PO}_4$  buffer (pH-7.8) comprising 0.05% NBT and 10 mM sodium azide for 1 h. After that the extract was boiled for 15 min at  $85^\circ\text{C}$ . The absorbance was recorded at 580 nm and expressed in  $\mu\text{mol g}^{-1} \text{ f.w.}$

### Assay of carbohydrates content

The total sugar content was measured using the protocol of Verma et al.<sup>23</sup> The ethanol (1ml) extract of shoot tissue was mixed with 4 ml of anthrone reagent (cold). Then the extract was boiled for 10 min and the absorbance was taken at 620 nm with expressed in  $\text{mg g}^{-1} \text{ f.w.}$  In addition, the reducing sugar content was determined by the protocol of Afzal et al.<sup>24</sup> In a similar manner, the ethanol extract (3 ml) of shoot tissue was added to 3 ml of 3,5-dinitro-salicylic acid (DNSA) solution. The mixture was heated for 5 min and 1 ml of a 40% sodium potassium tartrate solution was added for stabilization. After cooling, the content was read at 515 nm and denoted in  $\text{mg g}^{-1} \text{ f.w.}$  Moreover, the content of non-reducing sugar was estimated by deducting the reducing sugars from the total soluble sugar content. According to Parida et al.,<sup>25</sup> the starch content was determined by mixing the residues of alcoholic extracts of the shoot tissues with 5 ml of 52% perchloric acid (PCA) for 1 h. 1 ml of the PCA extract was added to 3 ml of anthrone solution. The PCA mixtures were boiled for 7.5 min and then read the color intensity at 630 nm. The starch content was estimated from the standard curve of glucose in a range of 0-100  $\mu\text{g mL}^{-1}$  and denoted as  $\text{mg g}^{-1} \text{ f.w.}$

### Assay of nucleic acid content

DNA was estimated following the method described by Lajmi.<sup>26</sup> The nucleic acid extract (1.5 ml) of each shoot tissues was mixed with diphenylamine solution (0.3 ml) separately, and kept in water bath at  $55^\circ\text{C}$  for 15 min. Then the absorbance of the extracts was recorded at 610

nm using a standard curve for standard DNA and denoted in  $\text{mg g}^{-1}$  f.w. Similarly, the RNA was also estimated adopting the technique of Lajmi.<sup>26</sup> The nucleic acid extract (1.5 ml) was mixed with 3 ml of orcinol reagent. Then the extracts were boiled at  $55^{\circ}\text{C}$  for 20 min and the absorbance was read at 660 nm. The RNA content was also assessed using the assistance of a standard curve prepared with standard RNA (20 to  $100 \mu\text{g ml}^{-1}$ ) and denoted in  $\text{mg g}^{-1}$  f.w.

#### Assay of POD activity

1.0 g of fresh shoot tissue was grinded with 0.1 M  $\text{K}_3\text{PO}_4$  buffer (pH-6.6), and the homogenates were centrifuged at 18000 rpm for 15 min at  $4^{\circ}\text{C}$ . Following Kaur et al.,<sup>27</sup> the enzyme extract was mixed with 3 ml of a 0.05 M pyrogallol reagent, and the mixture was then incubated at  $4^{\circ}\text{C}$  for 10 min. The reaction mixture was added to 0.5 ml of  $\text{H}_2\text{O}_2$  (0.5%) reagent, followed by incubation for 5 min. Then the absorbance was recorded at 420 nm and expressed in  $\text{mmol guaicol min}^{-1} \text{g f.w.}$

#### Assay of SA content

0.2 g of shoot tissues were homogenized with 95% ethanol and vortexed at 2500 rpm for 15 min at  $4^{\circ}\text{C}$ . The homogenates were mixed with 1 ml of 1% ferric chloride to estimate salicylic acid following the protocol of Naaz et al.<sup>28</sup> The

absorbance of supernatants was recorded at 540 nm and expressed as  $\text{mg g}^{-1}$  f.w.

#### Total phenolic contents

0.5 g shoot tissues were crushed using 80% cold methanol and the extracts were vortexed at 10000 rpm at  $4^{\circ}\text{C}$  for 20 min. The reaction solution was read at 280 nm using the Folin–Ciocalteu reagent, regarding the protocol of Dai et al.<sup>29</sup> and estimated from the standard curve of gallic acid and denoted in  $\text{mg g}^{-1}$  f.w.

#### Assay of PPO activity

According to the protocol of Elsheery et al.,<sup>30</sup> PPO activity was measured by the homogenization of 0.5 g of shoot tissue in 2 ml of 50 mM Tris-HCl (including 0.4 M sorbitol and 10 mM NaCl) (pH-7.2). The extracts were vortexed at 2000 rpm for 10 min, followed by mixing with 2.5 ml of 0.1 M  $\text{K}_3\text{PO}_4$  buffer (pH-6.5) and 0.3 ml of catechol reagent. The absorbance was recorded at 495 nm for every 30 sec up to 5 min and expressed as  $\text{U g}^{-1}$  f.w. The equation below can be used to determine the activity of PPO.

Enzyme units in the sample =  $K (\Delta A/\text{min})$   
where, K for catechol oxidase = 0.272

#### Statistical analysis

For the various parameters of WT and DPA seedlings, values are shown as the

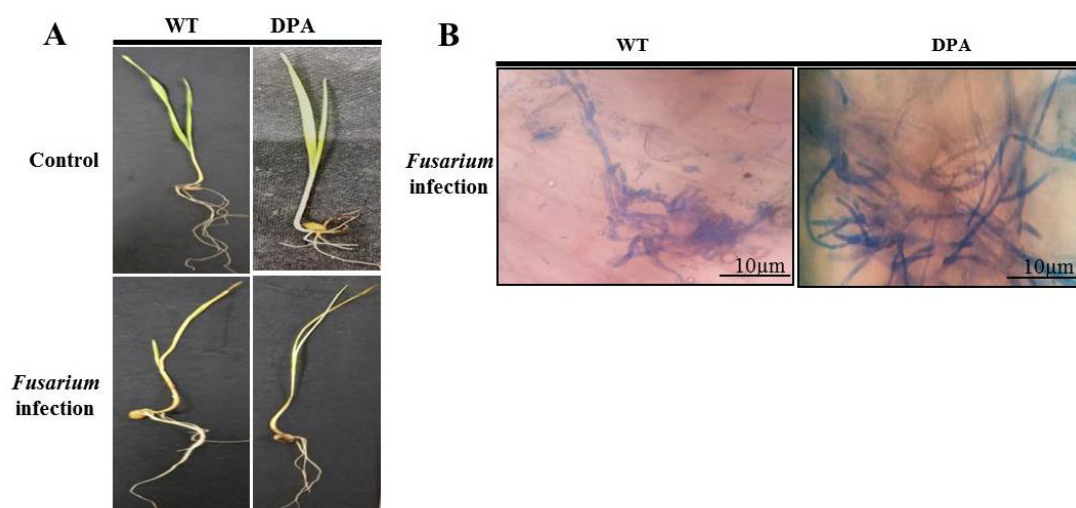


**Figure 1.** Plant phenotype and fungal growth A. WT and DPA under control and *Fusarium* infection, B. Mycelial growth

mean of three replicates. Here, the average of three replicates denotes the "mean of three independent seedlings," following the Student's t-test. Significance was defined as  $p \leq 0.05$  (\*). Data was given as mean  $\pm$  standard error of mean (SEM). The graph was performed using the GraphPad Prism software.

## RESULTS

### Morphological and anatomical analysis of WT and DPA shoots under stress condition

The leaves' surface area shrunk, their edges curled inward, and they wilted and became yellow due to chlorosis and stunted growth in DPA, while all these symptoms observed to be less in

WT when exposed to *F. oxysporum*. However, the WT and DPA exhibited less vigor and growth under the stress condition than under the non-stress condition (Figure 1A). In another investigation, the lactophenol cotton blue staining of shoots displayed fungal mycelial pattern present within the infected seedlings. An enhanced accumulation of fungal mycelia was found in DPA, which is indicative of high disease severity (Figure 1B).

The internal structure of the wheat shoot organ was studied under stress condition, which indicates the severity of damage at the tissue level. Figure 2A revealed that the disintegrated and reduced VBs in WT and DPA under stress condition compared to non-stress condition. In addition, the mechanical tissue like sclerenchyma

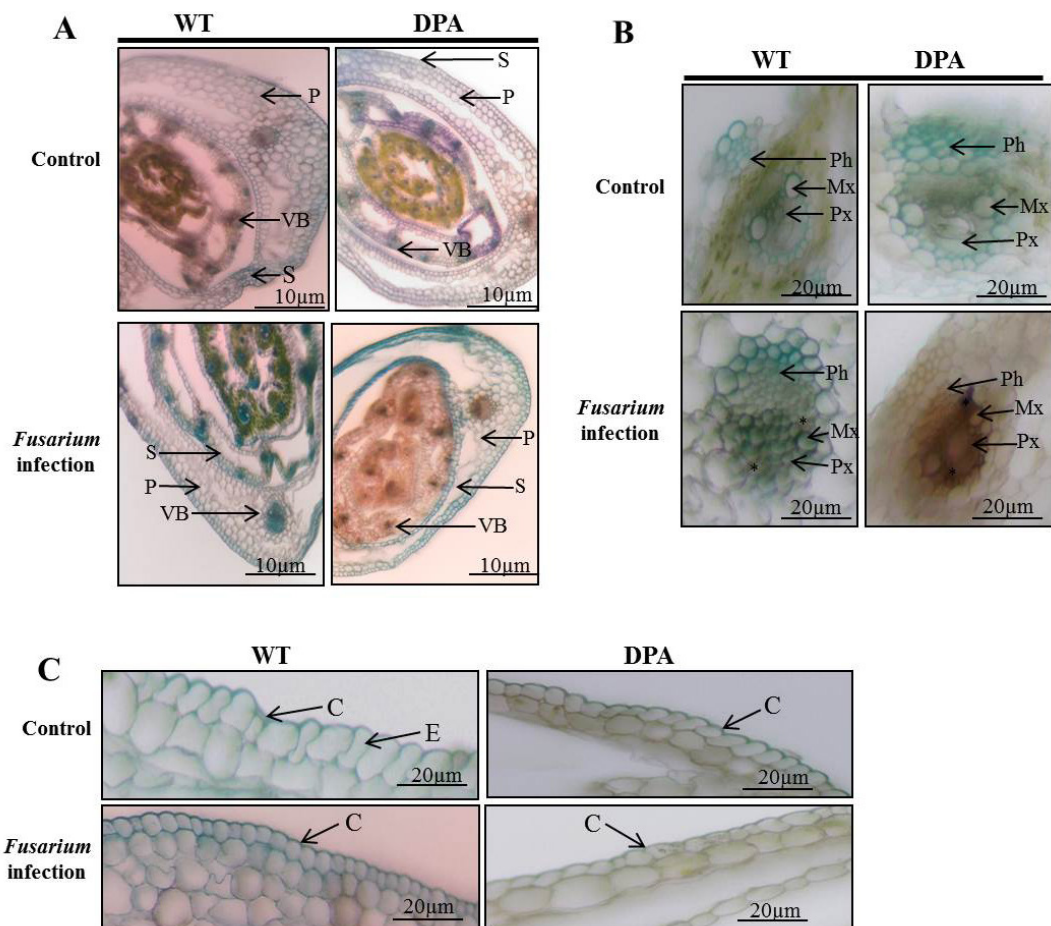


**Figure 2.** Histological analysis of internal structure A. TS of shoot, B. VBs, C. Epidermal layer. \* indicate the amorphous materials. Abbreviations: P- parenchyma; VB- vascular bundle; S- sclerenchyma; Ph- phloem; Mx- metaxylem; Px- protoxylem; C- cuticle; E- epidermis.



was conferred resistance against fungal infection due to its thickened lignified cell wall. The blue-green colored sclerenchyma cells were increased

in WT as compared to DPA. Moreover, the parenchyma cells were disorganized more in DPA than WT in response to stress condition. The Xy

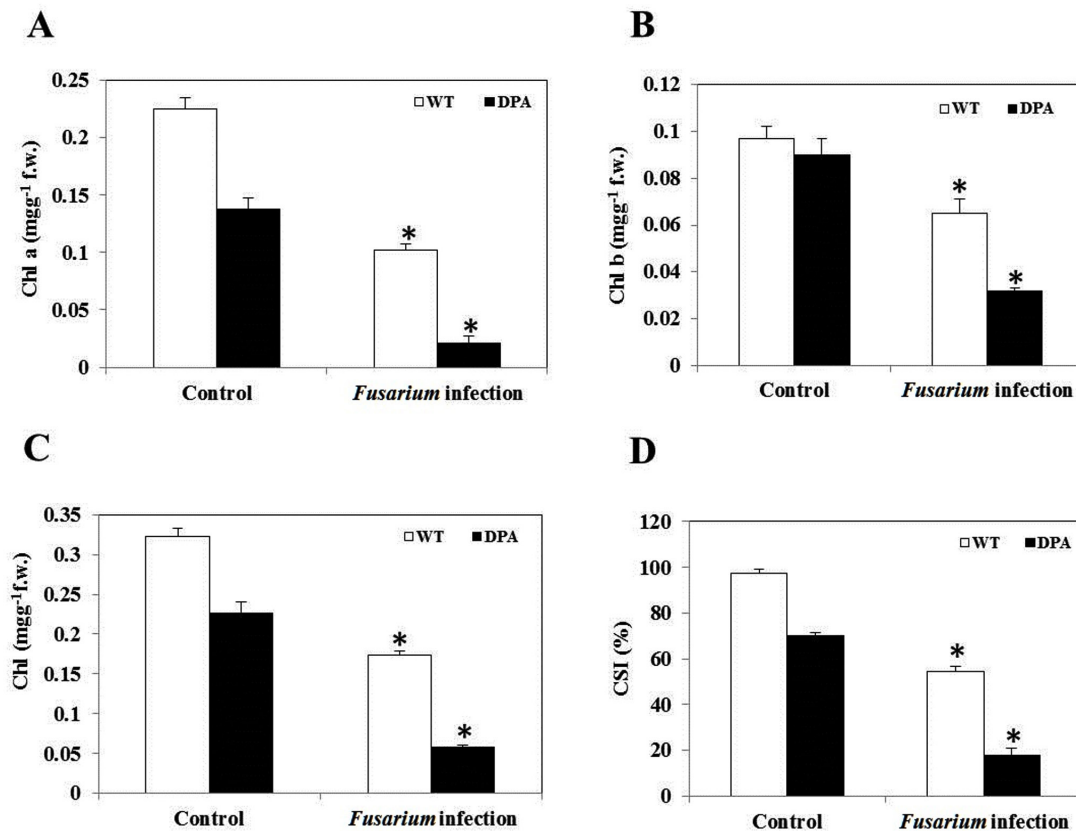


Figure 3. Photosynthetic pigments A. Chl a, B. Chl b, C. Chl, D. CSI (%)

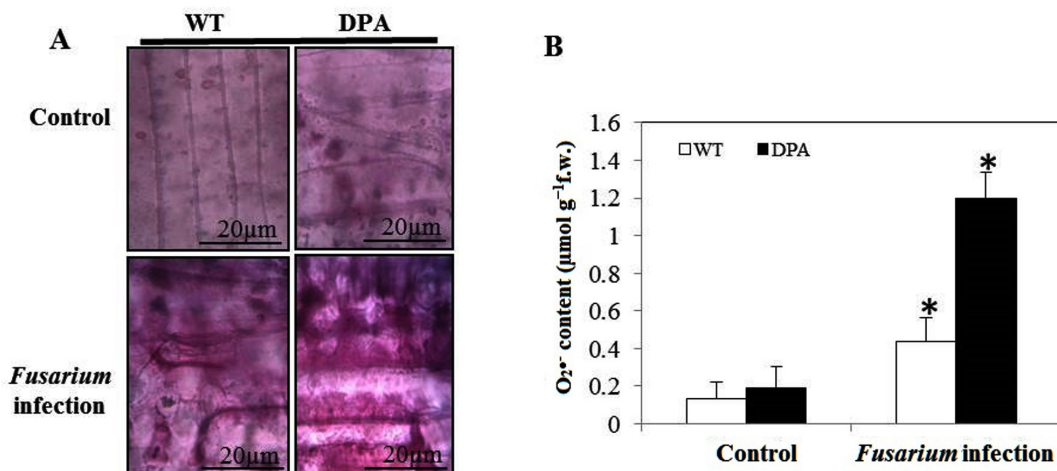


Figure 4. In vitro formation of O<sub>2</sub>•<sup>-</sup>. A. Localization of O<sub>2</sub>•<sup>-</sup>. B. O<sub>2</sub>•<sup>-</sup> content

and phloem (Ph) are the conducting tissues, which translocate nutrients from the source to sink cells. Under stress condition, the numbers of Xy (green) and Ph (red) cells were lower in DPA than WT. The metaxylem (Mx) and protoxylem (Px) were studied under stress condition to learn about the water transportation process, which reflects the metabolic activity including photosynthesis and transpiration in the shoot. The Mx, and Px were observed to be disintegrated in DPA than WT during stress condition. In addition, some amorphous materials were deposited in WT and

DPA under the stress condition (Figure 2B). In another investigation, a protective cutin and wax-made cuticle layer was studied for its inhibitory role against fungal invasion under stress condition. The cuticle layer of the epidermis increased in WT but decreased in DPA (Figure 2C).

### Photosynthetic pigments and their stability during stress condition

Chlorophyll (Chl) is a photosynthetic component that is utilized in the light-harvesting metabolic process, including the light reaction and

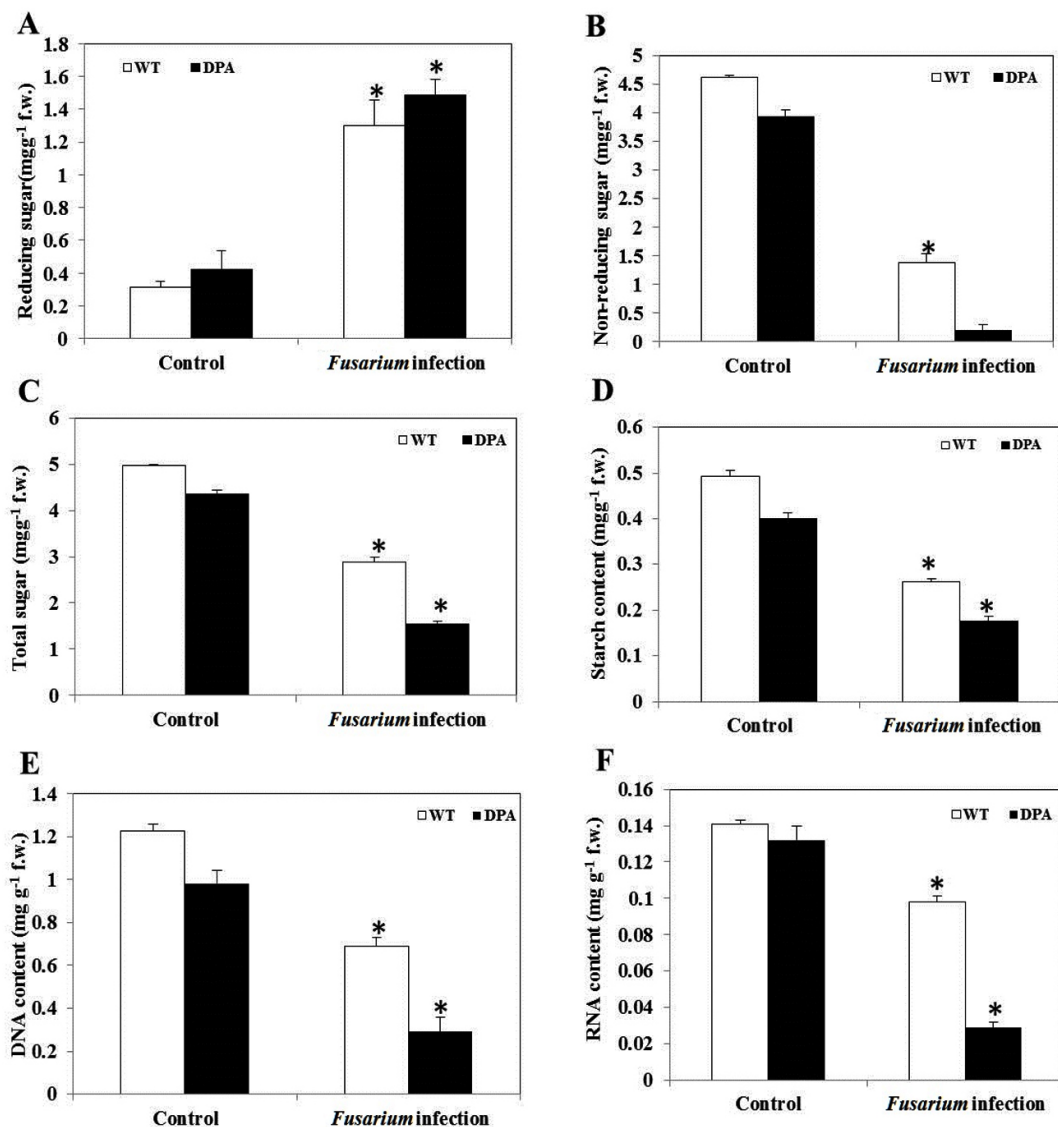


**Figure 5.** Macromolecules content A. Reducing sugar, B. Non-reducing sugar, C. Total sugar, D. Starch, E. DNA, and F. RNA

the Calvin cycle. It converts inorganic compounds into organic compounds. *Fusarium*-induced oxidative stress caused a decrease in chl content under stress condition. The Chl a was decreased by 1.64- and 3.5-fold in WT and DPA (Figure 3A), whereas the Chl b decreased by 1.9- and 0.48-fold in WT and DPA under the stress condition as compared to the non-stress condition (Figure 3B). Overall, the Chl content decreased 2.4- and 1.4- fold in WT, and DPA under stress condition (Figure 3C). The potential of plants to resist stress is assessed by the chlorophyll stability index (CSI). A low CSI value means that the photosynthetic system was affected by stress. Our results showed that the CSI was decreased by 1.6- and 4.6-fold in WT and DPA under the stress condition, respectively, compared to the non-stress condition (Figure 3D).

#### Accumulation of $O_2^{\bullet-}$ in response to *Fusarium* infection

The  $O_2^{\bullet-}$  content, an indicator of oxidative damage due to imbalance of redox system,

was estimated in both WT and DPA exposed to *Fusarium* infection. No significant visual difference was seen in the accumulation of  $O_2^{\bullet-}$  in WT and DPA under non-stress condition. The DPA showed increased accumulation of  $O_2^{\bullet-}$  as dark blue-purple spots as compared to WT under the stress condition (Figure 4A). Furthermore, the  $O_2^{\bullet-}$  content was increased by 4.0- and 6.0-fold in WT and DPA (Figure 4B).

#### Photoassimilates and nucleic acid content in infected seedlings

Carbohydrates are the product of the photosynthesis process. It has a crucial role in the formation of organic compounds, serves as a building block for cell wall synthesis and different metabolic pathways, and also acts as a storage food material found in parenchymatous tissues. Changes in the total sugar content in the shoot of wheat under *Fusarium*-induced oxidative stress were examined. When compared to both conditions, WT and DPA showed an increased reducing sugar content of 5.2 and 4.2-fold,

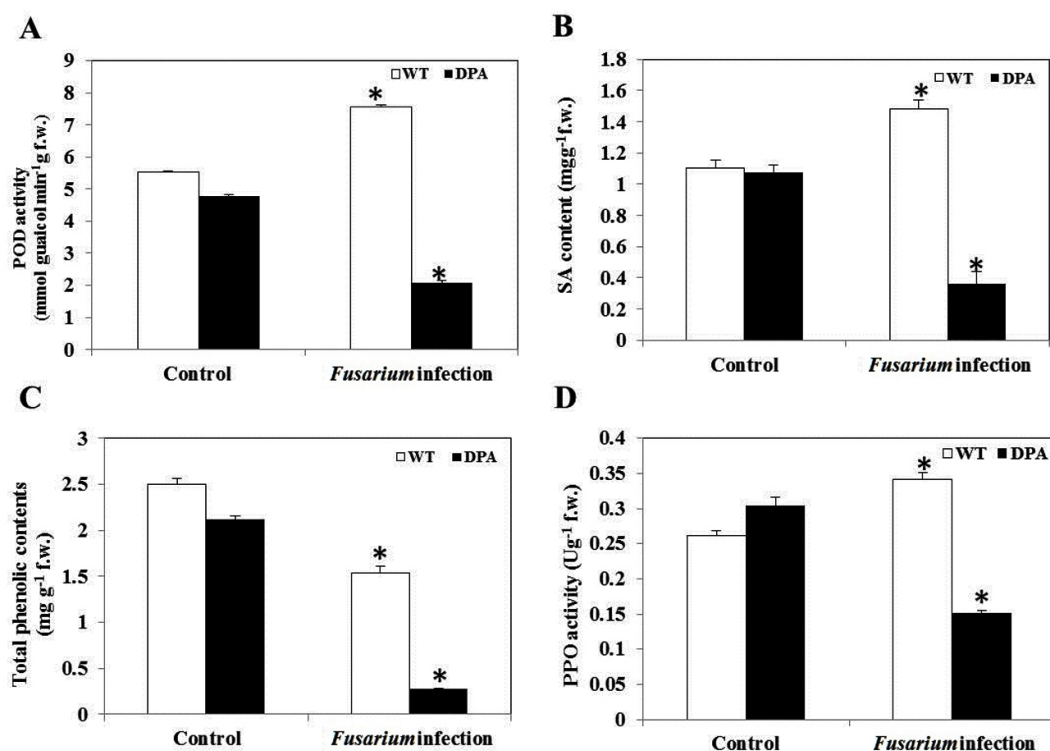


**Figure 6.** Secondary metabolites and antioxidant enzyme activity A. POD, B. SA, C. Total phenolics, D. PPO



respectively (Figure 5A), whereas non-reducing sugar decreased in WT and DPA by 3.1- and 9.75-fold under the stress condition (Figure 5B). In addition, the total sugar content was decreased in WT and DPA by 1.56- and 2.93-fold, respectively, in the stress condition (Figure 5C). In another investigation, the starch content was reduced to 1.68 and 1.9-fold in WT and DPA under stress condition (Figure 5D).

DNA and RNA structure and function have a key role in antioxidant enzyme regulation during fungal infection.<sup>31</sup> The present study revealed that the DNA content decreased by 1.71- and 3.33-fold, respectively, in WT and DPA under stress conditions as compared to the non-stress condition (Figure 5E), due to the high rate of DNA degradation during pathogen infection.<sup>32</sup> Moreover, the DNA repair genes were modified during infection by promoting DNA instability in plants.<sup>33</sup> Furthermore, the RNA content was decreased by 1.4- and 1.3-fold in WT and DPA under stress conditions (Figure 5F).

#### Level of SA and phenolics in WT compared to DPA during *Fusarium* infection

SA is a naturally occurring defensive phenolic compound that alleviates a high level of oxidative stress. Under *Fusarium* infection, plants lower ROS by inducing SA for proper operation, which is accompanied by a considerable rise in the activities of antioxidant enzymes, i.e., PPO and POD, under stress condition.<sup>34</sup> The POD activity was increased by 1.45-fold in WT and decreased by 2.4-fold in DPA, respectively, under the stress condition (Figure 6A). In addition, there was no remarkable difference in the specific content of SA in WT and DPA under non-stress condition. However, a significant increase of 1.36-fold occurred in WT in contrast to DPA, where the reduction was 3.3-fold in response to infection (Figure 6B). In addition, the phenolics decreased by 1.6- and 6.6-fold in WT and DPA, respectively (Figure 6C). Furthermore, the WT showed an increase (1.4-fold) in PPO activity and a decrease (2.0-fold) in DPA under stress condition (Figure 6D).

## DISCUSSION

*Fusarium*-induced wilt disease is one of the biotic stress factors that could reduce the growth

and development of plants. The infection may interfere with different biosynthetic pathways and retard plant growth and yield. Various studies have reported the pathogenetic effect of exogenously applying *F. oxysporum* spores to the plants.<sup>35</sup> In the present study, *Fusarium* exposure exhibited more yellowing and wilting in DPA in contrast to WT. The severity of wilting occurred due to blockage of xylem vessels with progressive growth of *F. oxysporum* in leaves and shoots and reduction of Chl contents, which eventually leads to death.<sup>36</sup> Moreover, the enhanced fungal mycelia found in the shoots of DPA-treated wheat seedlings exposed to *Fusarium* demonstrates the system's inability to block pathogen entrance.

Many reports have stated that the anatomical features of wheat stems have steadily deteriorated due to *Fusarium* infection.<sup>37,38</sup> The VBs acted as a conducting system to provide sap throughout the vegetative organs of plants. The Xy is affected by the endophytic *F. oxysporum* resulting interruption at the translocation system.<sup>39</sup> The VBs of WT and DPA were damaged and collapsed due to fungal growth, similarly, the roots and stems of corn plants were infected by a pathogenic strain of *F. verticillioides*.<sup>40</sup> In addition, the sclerenchyma cells provide mechanical support to VBs through thickening primary cell walls, which further acts as a mechanical barrier against fungal invasion. The present study revealed higher numbers of sclerenchyma cells in WT as compared to DPA during *Fusarium* infection. The size and thickness of sclerenchyma cells were increased in corn plants. This can be noticed as defending plant tissues against infection by an endophytic *F. sacchari*.<sup>41</sup> The treatment with 2,4-D induced the reduction of sclerenchyma cells in wheat seedlings during *Fusarium* infection. Moreover, the parenchyma cells conduct most of the metabolic activity, such as the photosynthesis process, and serve as a carbohydrate storage compartment while also providing support to the vascular system. The parenchyma cells were observed to be lower in DPA than WT. Similarly, these cells were also distorted, fragmented, and collapsed in *Macrophomina phaseolina* infected mungbean plants.<sup>42</sup>

The Mx and Px cells are responsible for the storage and long-distance transport of sap, whereas the Ph tissue translocates soluble

sugars to all organs of the plant. The Mx, Px, and Ph cells were observed to have reduced and irregular sizes in DPA as compared to WT, due to the blockage of translocation systems. Chen et al.,<sup>43</sup> reported that the reduced area of Mx and Px were observed in the roots, stems and leaves of wild barley (*Hordeum brevisubulatum*) infected by a *Epichloe bromicola* pathogen, and also in infected kallar grass and faba beans,<sup>44</sup> and sorghum during infection.<sup>45</sup> In the present study, the deposition of amorphous material in the VBs indicated the response of hyphal proliferation in WT and DPA shoot tissues. Nevertheless, the DPA showed pathogen colonization and produced more amorphous materials. da Conceição et al.<sup>46</sup> reported the evidence of phenolic-like compounds as amorphous materials produced in rice against *Pyricularia oryzae*. In addition, the cuticle layer was thick in WT, which indicates the enhanced SA and phenolic contents in response to fungal mycelium.<sup>47</sup> In another investigation, DPA showed a reduced cuticle layer due to lower content of SA, phenolics, and antioxidant enzyme activity.<sup>48</sup>

The Chl a and Chl b content were declined in *Malus pumila* Mill. leaves, resulting in reduced photosynthetic activity during apple phytoplasma infection.<sup>49</sup> Our study indicated that Chl a, Chl b, and Chl were decreased in DPA as compared to WT during *Fusarium* infection.<sup>50</sup> Aybeke<sup>10</sup> have investigated that total Chl content was declined due to *Fusarium* infection in several plants due to damage to pigments, the photosystems complex, and chloroplast membranes. Further, the Chl could be harmed by  $O_2\bullet^-$  leads to progressive chlorosis, dysfunction of PSI and PSII in chloroplasts, and cell death,<sup>51</sup> also reduces the sugar contents in parenchymatous cells of coconut palms, maize, and papaya leaves.<sup>52</sup> The results indicate that the inoculation of *Fusarium* enhances the pathogenesis of wheat seedlings, affecting growth and development.

Wilt disease induces the rapid accumulation of  $O_2\bullet^-$ , which is used to measure the injuries in the plants. In the present study,  $O_2\bullet^-$  accumulation was increased in DPA than WT during *Fusarium* infection. In addition, the damaged tissues also produced more ROS during infection. Moreover, the  $O_2\bullet^-$  impart photosynthesis apparatus and reduces the level of carbohydrates (primary metabolites) that serve as the progenitor

for the synthesis of secondary metabolites (such as phenolic compounds) that inhibit the entry of fungal hyphae.<sup>13</sup>

The reducing sugar was abundant in WT and DPA during infection; similarly, the reducing carbohydrates were produced in the susceptible cv. Widusa.<sup>53</sup> In contrast, the non-reducing sugar was low in WT and DPA under stress condition. The photosynthates were reduced in *Phaseolus vulgaris* plants infected with *Colletotrichum lindemuthianum* and *Uromyces appendiculatus*.<sup>54</sup> In many plants, *Fusarium* infection is achieved by increasing the deposition of soluble sugars.<sup>55</sup> These chemical substances are crucial for osmotic adjustment as well as for protecting membranes and biomolecules.<sup>56</sup> In contrast, the total sugar and starch content of both the WT and DPA decreased under stress condition as compared to non-stress condition. Scarpari et al.<sup>57</sup> stated that the production of total soluble carbohydrates was reduced in *Theobroma cacao* plants infected with *Crinipellis pernicioso*, and also in sunflower (*Helianthus annuus* L.) infected with sunflower chlorotic mottle virus,<sup>58</sup> and leaves and stems of infected papaya plants.<sup>59</sup> These results suggested that the osmotic adjustment was greater in WT than DPA, indicating the structural disorganization of parenchyma cells. The present study revealed that DNA and RNA content were decreased in WT and DPA under stress condition, similarly reported in *Ralstonia solanacearum* infected transgenic tobacco plants,<sup>60</sup> and also in *Meloidogyne incognita* infected tomato plants due to increase rate of ribonuclease activity.<sup>61</sup> Further, Zahm et al.<sup>62</sup> showed 2,4-DPA induced the reduction of DNA and RNA content, leading to disorganised growth and death in etiolated soybean seedlings.

In plant species, POD and PPO are part of a sophisticated antioxidant defense system that removes ROS. These antioxidant enzymes are essential for removing these harmful substances from cells and reducing ROS-induced oxidative cell damage.<sup>63</sup> In the present study, POD was increased in WT, this implies the protection from oxidative damage and reduced in immunocompromised DPA during *Fusarium* infection.<sup>64</sup> In addition, SA acts as a signal molecule for conferring resistance against fungal attack. Our results stated that, SA was increased in WT indicating the synthesis of phenolics that minimizes the

O<sub>2</sub>•- to provide protection from fungal infection and the DPA reduced the SA related compounds in the plants under the stress condition due to inhibition of PAL activity.<sup>65</sup> SA induces the phenolic compounds, which are known to be maintaining cell wall strengthening in Xy and Ph tissues. Phenolics play a prime role in lignin and pigment biosynthesis, providing structural integrity and support to plants by inhibiting fungal entry. The aggregation of the phenolic monomers were required for sclerenchyma and Xy lignification with the involvement of both PPO and POD.<sup>32</sup> In an investigation, the phenolic contents were increased in WT, which consistent with SA but reduced in DPA under stress condition, and concomitant to rust diseased plants.<sup>65</sup> Moreover, the PPO activity was enhanced in WT after pathogen colonization, which was concomitant with the oxidizing phenolic compounds in tomato plants with enhanced PPO activity against bacterial canker disease.<sup>66</sup> Therefore, the alternation of production of SA and phenolics induces structural disorganization which facilitate the fungal proliferation. Vago et al.<sup>67</sup> was also reported the pathogen-induced biochemical and anatomical changes in *Lotus tenuis*.

## CONCLUSION

In conclusion, 1 mM DPA treatment significantly altered the anatomical and biochemical aspects of wheat seedlings, which resulted in an increase susceptibility against *F. oxysporum*. Thus, the increase in susceptibility may be due to the structural disorganization and low level of secondary metabolites, which serves as an innate immunity against fungal pathogens. Further studies are required to unravel the molecular mechanisms underlying wheat host susceptible to *Fusarium* attack that can be used in future to counter the susceptibility.

## ACKNOWLEDGEMENTS

The authors would like to thank P.G. Department of Biosciences and Biotechnology, Fakir Mohan University, Balasore, Odisha, India, for providing the necessary laboratory facilities to carry out the study.

## CONFLICT OF INTEREST

The authors declare that there is no conflict of interest.

## AUTHORS' CONTRIBUTION

All authors listed have made a substantial, direct and intellectual contribution to the work, and approved it for publication.

## FUNDING

None.

## DATA AVAILABILITY

All datasets generated or analyzed during this study are included in the manuscript.

## ETHICS STATEMENT

Not applicable.

## REFERENCES

1. Malhi GS, Kaur M, Kaushik P, Alyemeni MN, Alsahli AA, Ahmad P. Arbuscular mycorrhiza in combating abiotic stresses in vegetables: An eco-friendly approach. *Saudi J Biol Sci.* 2021;28(2):1465-1476. doi: 10.1016/j.sjbs.2020.12.001
2. Sampaio AM, Araujo SDS, Rubiales D, VazPatto MC. *Fusarium* wilt management in legume crops. *Agronomy.* 2020;10(8):1073. doi: 10.3390/agronomy10081073
3. Hussain A, Ahmad M, Nafees M, et al. Plant-growth-promoting *Bacillus* and *Paenibacillus* species improve the nutritional status of *Triticum aestivum* L. *PLoS One.* 2020;15(12):e0241130. doi: 10.1371/journal.pone.0241130
4. Gabrekiristos E., Demiyo T. Hot pepper *Fusarium* wilt (*Fusarium oxysporum* f. sp. *capsici*): Epidemics, characteristic features and management options. *J Agric Sci.* 2020;12(10):347-360. doi: 10.5539/jas.v12n10p347
5. Garces-Fiallos FR, de Borba MC, Schmidt EC, Bouzon ZL, Stadnik MJ. Delayed upward colonization of xylem vessels is associated with resistance of common bean to *Fusarium oxysporum* f. sp. *phaseoli*. *Eur J Plant Pathol.* 2017;149(2):477-489. doi: 10.1007/s10658-017-1197-6
6. Abou El-ghit HM. Impact of Post-Emergence Application of Dichlorophenoxy Acetic Acid (2,4-D) Herbicide on Growth and Development of Three Weeds Associated with Maize Growth. *Int J Curr Microbiol App Sci.* 2016;5(2):794-801. doi: 10.20546/ijcmas.2016.502.090
7. Li P, Liu W, Zhang Y, et al. Fungal canker pathogens trigger carbon starvation by inhibiting carbon metabolism in poplar stems. *Sci Rep.* 2019;9(1):1-14. doi: 10.1038/s41598-019-46635-5

8. Rose RJ. Contribution of massive mitochondrial fusion and subsequent fission in the plant life cycle to the integrity of the mitochondrion and its genome. *Int J Mol Sci.* 2021;22(11):5429. doi: 10.3390/ijms22115429
9. Garcia-Viera MA, Sanchez-Segura L, Chavez-Calvillo G, Jarquin-Rosales D, Silva-Rosales L. Changes in leaf tissue of Carica papaya during single and mixed infections with Papaya ringspot virus and Papaya mosaic virus. *Biologia Plantarum.* 2018;62(1):173-180. doi: 10.1007/s10535-017-0741-8
10. Aybeke M. *Fusarium* infection causes genotoxic disorders and antioxidant-based damages in *Orobancha* spp. *Microbiol Res.* 2017;201:46-51. doi: 10.1016/j.micres.2017.05.001
11. Minh-Thu PT, Kim JS, Chae S, et al. A WUSCHEL homeobox transcription factor, OsWOX13, enhances drought tolerance and triggers early flowering in rice. *Molecules and Cells.* 2018;41(8):781-798.
12. Li C, Ma D, Chen M, et al. Ulinastatin attenuates LPS-induced human endothelial cells oxidative damage through suppressing JNK/c-Jun signaling pathway. *Biochem Biophys Res Commun.* 2016;474(3):572-578. doi: 10.1016/j.bbrc.2016.04.104
13. Tyagi P, Singh A, Gupta A, Prasad M, Ranjan R. Mechanism and function of salicylate in plant toward biotic stress tolerance. *Emerging Plant Growth Regulators in Agriculture.* 2022;131-164. doi: 10.1016/B978-0-323-91005-7.00018-7
14. Lee MH, Jeon HS, Kim SH, et al. Lignin-based barrier restricts pathogens to the infection site and confers resistance in plants. *The EMBO J.* 2019;38(23):201948. doi: 10.15252/embj.2019101948
15. Dordas C. Role of nutrients in controlling plant diseases in sustainable agriculture. A review. *Agronomy for Sustainable Development.* 2008;28(1):33-46. doi: 10.1051/agro:2007051
16. Mittra B, Ghosh P, Henry SL, et al. Novel mode of resistance to *Fusarium* infection by mild dose pre-exposure of cadmium to wheat. *Plant Physiol Biochem.* 2004;42(10):781-787. doi: 10.1016/j.plaphy.2004.09.005
17. Flores-Caceres ML, Hattab S, Hattab S, Boussetta H, Banni M, Hernandez LE. Specific mechanisms of tolerance to copper and cadmium are compromised by a limited concentration of glutathione in Alfalfa plants. *Plant Sci.* 2015;233:165-173. doi: 10.1016/j.plantsci.2015.01.013
18. Charya LS, Garg S. Advances in methods and practices of ectomycorrhizal research. *Adv Biol Sci Res.* 2019:303-325. doi: 10.1016/B978-0-12-817497-5.00019-7
19. Parker GA, Li N, Takayama K, Farese AM, MacVittie TJ. Lung and heart injury in a nonhuman primate model of partial-body irradiation with minimal bone marrow sparing. Histopathological evidence of lung and heart injury. *Health Physics.* 2019;116(3):383-400. doi: 10.1097%2FHP.0000000000000936
20. Porra RJ. The chequered history of the development and use of simultaneous equations for the accurate determination of chlorophylls a and b. *Photosynth Res.* 2002;73(1):149-156. doi: 10.1023/A:1020470224740
21. Sairam RK, Deshmukh PS, Shukla DS. Tolerance of drought and temperature stress in relation to increased antioxidant enzyme activity in wheat. *J Agron Crop Sci.* 1997;178(3):171-178. doi: 10.1111/j.1439-037X.1997.tb00486.x
22. Pyngrope S, Bhoomika K, Dubey RS. Reactive oxygen species, ascorbate-glutathione pool, and enzymes of their metabolism in drought-sensitive and tolerant indica rice (*Oryza sativa* L.) seedlings subjected to progressing levels of water deficit. *Protoplasma.* 2013;250(2):585-600. doi: 10.1007/s00709-012-0444-0
23. Verma S, Dubey RS. Effect of cadmium on soluble sugars and enzymes of their metabolism in rice. *Biologia Plantarum.* 2001;44(1):117-123. doi: 10.1023/A:1017938809311
24. Afzal I, Rauf S, Basra SMA, Murtaza G. Halopriming improves vigor, metabolism of reserves and ionic contents in wheat seedlings under salt stress. *Plant Soil Environ.* 2008;54(9):382-388. doi: 10.17221/408-PSE
25. Parida AK, Das AB, Sanada Y, Mohanty P. Effects of salinity on biochemical components of the mangrove, *Aegiceras corniculatum*. *Aquatic Botany.* 2004;80(2):77-87. doi: 10.1016/j.aquabot.2004.07.005
26. Lajmi A, Bourven I, Joussein E, Simon S, Soubrand M, Medhioub M. DNA Detection After Interaction with Clay Minerals and Soils: An Analytical Approach. *Conference of the Arabian Journal of Geosciences Springer, Cham.* 2019:309-312. doi: 10.1007/978-3-030-72547-1\_66
27. Kaur P, Bali S, Sharma A, et al. Cd induced generation of free radical species in *Brassica juncea* is regulated by supplementation of earthworms in the drilosphere. *Sci Total Environ.* 2019;55:663-675. doi: 10.1016/j.scitotenv.2018.11.096
28. Naaz H, Yasin D, Afzal B, Sami N, Khan NJ, Fatma T. Exogenous salicylic acid mediated herbicide (Paraquat) resistance in cyanobacterial biofertilizer *Microchaete* sp. NCCU-342. *Environ Sci Pollut Res.* 2021;30(10):25069-25079. doi: 10.1007/s11356-021-15378-0
29. Dai T, Chen J, McClements DJ, et al. Protein-polyphenol interactions enhance the antioxidant capacity of phenolics: Analysis of rice glutelin-procyanidin dimer interactions. *Food & Function.* 2019;10(2):765-774. doi: 10.1039/C8FO02246A
30. Elsheery NI, Helaly MN, Omar SA, et al. Physiological and molecular mechanisms of salinity tolerance in grafted cucumber. *S Afr J Bot.* 2020;130:90-102. doi: 10.1016/j.sajb.2019.12.014
31. Lalwani Z, Kumar P. Oxidative stress in plants: A delicate balance between life and death. 2022.
32. Meriga B, Reddy BK, Rao KR, Reddy LA, Kishor PK. Aluminium-induced production of oxygen radicals, lipid peroxidation and DNA damage in seedlings of rice (*Oryza sativa*). *J Plant Physiol.* 2004;161(1):63-68. doi: 10.1078/0176-1617-01156
33. Covo S. Genomic instability in fungal plant pathogens. *Genes.* 2020;11(4):421. doi: 10.3390/genes11040421
34. Islam W, Tayyab M, Khalil F, Hua Z, Huang Z, Chen HY. Silicon-mediated plant defense against pathogens and insect pests. *Pestic Biochem Physiol.* 2020;168:104641. doi: 10.1016/j.pestbp.2020.104641

35. Oz M, Lorke DE, Hasan M, Petroianu GA. Cellular and molecular actions of Methylene Blue in the nervous system. *Med Res Rev*. 2011;31(1):93-117. doi: 10.1002/med.20177
36. Sun Y, Wang M, Li Y, Gu Z, Ling N, Shen Q, Guo S. Wilted cucumber plants infected by *Fusarium oxysporum* f. sp. cucumerinum do not suffer from water shortage. *Ann Bot*. 2017;120(3):427-436. doi: 10.1093/aob/mcx065
37. Shahid M, Ahmed B, Zaidi A, Khan MS. Toxicity of fungicides to *Pisum sativum*: a study of oxidative damage, growth suppression, cellular death and morpho-anatomical changes. *RSC Advances*. 2018;8(67):38483-38498. doi: 10.1039/C8RA03923B
38. Kretschmer M, Damoo D, Djamei A, Kronstad J. Chloroplasts and plant immunity: where are the fungal effectors? *Pathogens*. 2019;9(1):19. doi: 10.3390/pathogens9010019
39. Liu G, Chater KF, Chandra G, Niu G, Tan H. Molecular regulation of antibiotic biosynthesis in *Streptomyces*. *Microbiol Mol Biol Rev*. 2013;77(1):112-143. doi: 10.1126/sciadv.aaz0478
40. Rashad YM, Abdalla SA, Shehata AS. *Aspergillus flavus* YRB2 from *Thymelaea hirsuta* (L.) Endl., a non-aflatoxigenic endophyte with ability to overexpress defense-related genes against *Fusarium* root rot of maize. *BMC Microbiol*. 2022;22(1):1-14. doi: 10.1186/s12866-022-02651-6
41. Terna TP, Mohamed Nor NMI, Zakaria L. Histopathology of Corn Plants Infected by Endophytic Fungi. *Biology*. 2022;11(5):641. doi: 10.3390/biology11050641
42. Khan IH, Javaid A. Biocontrol *Aspergillus* species together with plant biomass alter histochemical characteristics in diseased mungbean plants. *Microsc Res Tech*. 2022;85(8):2953-2964. doi: 10.1002/jemt.24145
43. Chen T, White JF, Li C. Fungal endophyte *Epichloe bromicola* infection regulates anatomical changes to account for salt stress tolerance in wild barley (*Hordeum brevisubulatum*). *Plant and Soil*. 2021;461(1):533-546. doi: 10.1007/s11104-021-04828-w
44. Nassar RM, Kamel HA, Ghoniem AE, et al. Physiological and anatomical mechanisms in wheat to cope with salt stress induced by seawater. *Plants*. 2020;9(2):237. doi: 10.3390/plants9020237
45. Shalaby TA, Taha NA, Taher DI, et al. Paclobutrazol improves the quality of tomato seedlings to be resistant to *Alternaria solani* Blight disease: Biochemical and histological perspectives. *Plants*. 2022;11(3):425. doi: 10.3390/plants11030425
46. da Conceicao EGJ, Martins FM, de Aguiar Accioly AM, de Freitas-Silva L, da Cruz MFA. Histological changes in banana rhizomes promoted by a silicon-*Fusarium oxysporum* interaction. *J Plant Pathol*. 2021;103(2):531-537. doi: 10.1007/s42161-021-00778-5
47. Lim GH, Liu H, Yu K, et al. The plant cuticle regulates apoplastic transport of salicylic acid during systemic acquired resistance. *Science Advances*. 2020;6(19):0478. doi: 10.1126/sciadv.aaz0478
48. Maghoumi M, Amodio ML, Fatchurrahman D, Cisneros-Zevallos L, Colelli G. Pomegranate husk scald browning during storage: a review on factors involved, their modes of action, and its association to postharvest treatments. *Foods*. 2022;11(21):3365. doi: 10.3390/foods11213365
49. Bertamini MASSIMO, Grando MS, Nedunchezian N. Effects of phytoplasma infection on pigments, chlorophyll-protein complex and photosynthetic activities in field grown apple leaves. *Biologia Plantarum*. 2003;47(2):237-242. doi: 10.1023/B:BIOP.0000022258.49957.9a
50. Guoth A, Tari I, Galle A, et al. Comparison of the drought stress responses of tolerant and sensitive wheat cultivars during grain filling: changes in flag leaf photosynthetic activity, ABA levels, and grain yield. *J Plant Growth Regul*. 2009;28(2):167-176. doi: 10.1007/s00344-009-9085-8
51. Zavafer A, Gonzalez-Solls A, Palacios-Bahena S, et al. Organized disassembly of photosynthesis during programmed cell death mediated by long chain bases. *Sci Rep*. 2020;10(1):1-14. doi: 10.1038/s41598-020-65186-8
52. Oropeza-Salin C, Saenz L, Narvaez M, et al. Dealing with lethal yellowing and related diseases in coconut. *Coconut Biotechnology: Towards the Sustainability of the 'Tree of Life*. 2020;169-197. doi: 10.1007/978-3-030-44988-9\_9
53. Sadohara R. Quality characteristics of bean paste as a confectionery ingredient and recent breeding efforts of common beans in Japan. *J Sci Food Agric*. 2020;100(1):10-15. doi: 10.1002/jsfa.10013
54. Perez-Bueno ML, Pineda M, Baron M. Phenotyping plant responses to biotic stress by chlorophyll fluorescence imaging. *Front Plant Sci*. 2019;10:1135. doi: 10.3389/fpls.2019.01135
55. Abdellatif MA, Elagamey E, Kamel SM. Chitosan is the ideal resource for plant disease management under sustainable agriculture. 2022. doi: 10.5772/intechopen.107958
56. Mostajeran A, Rahimi-Eichi V. Effects of drought stress on growth and yield of rice (*Oryza sativa* L.) cultivars and accumulation of proline and soluble sugars in sheath and blades of their different ages leaves. *Am Eurasian J Agric Environ Sci*. 2009;5(2):264-272.
57. Scarpari LM, Meinhardt LW, Mazzafera P, et al. Biochemical changes during the development of witches broom: the most important disease of cocoa in Brazil caused by *Crinipelis perniciosa*. *J Exp Bot*. 2005;56(413):865-877. doi: 10.1093/jxb/eri079
58. Arias MC, Lenardon S, Taleisnik E. Carbon metabolism alterations in sunflower plants infected with the Sunflower chlorotic mottle virus. *J Phytopathol*. 2003;151(5):267-273. doi: 10.1046/j.1439-0434.2003.00718.x
59. Soni SK, Mishra MK, Mishra M, et al. Papaya Leaf Curl Virus (PaLCuV) Infection on Papaya (*Carica papaya* L.) Plants alters anatomical and physiological properties and reduces bioactive components. *Plants*. 2022;11(5):579. doi: 10.3390/plants11050579
60. Ceccherini M, Pote J, Kay E, et al. Degradation and transformability of DNA from transgenic leaves. *Appl Environ Microbiol*. 2003;69(1):673-678. doi: 10.1128/AEM.69.1.673-678.2003
61. Vos C, Schouteden N, van Tuinen D, et al. Mycorrhiza-



- induced resistance against the root-knot nematode *Meloidogyne incognita* involves priming of defense gene responses in tomato. *Soil Biol Biochem.* 2013;60:45-54. doi: 10.1016/j.soilbio.2013.01.013
62. Zahm SH, Weisenburger DD, Babbitt PA, et al. A case-control study of non-Hodgkin's lymphoma and the herbicide 2, 4-dichlorophenoxyacetic acid (2, 4-D) in eastern Nebraska. *Epidemiology.* 1990;1(5):349-356. doi: 10.1097/00001648-199009000-00004
63. Alpoz AR, Tosun N, Eronat C, Delen N, Sen BH. Effects of 2, 4-dichlorophenoxy acetic acid dimethyl amine salt on dental hard tissue formation in rats. *Envion Int.* 2001;26(3):137-142. doi: 10.1016/S0160-4120(00)00095-7
64. Valletta A, Iozia LM, Leonelli F. Impact of environmental factors on stilbene biosynthesis. *Plants.* 2021;10(1):90. doi: 10.3390/plants10010090
65. Kunej U, Mikulic-Petkovsek M, Radisek S, Stajner N. Changes in the phenolic compounds of hop (*Humulus lupulus* L.) Induced by infection with *Verticillium nonalfalfae*, the causal agent of hop *Verticillium* wilt. *Plants.* 2020;9(7):841. doi: 10.3390/plants9070841
66. Tripathi R, Vishunavat K, Tewari R, et al. Defense inducers mediated mitigation of bacterial canker in tomato through alteration in oxidative stress markers. *Microorganisms.* 2022;10(11):2160. doi: 10.3390/microorganisms10112160
67. Vago ME, Jaurena G, Estevez JM, Castro MA, Zavala JA, Ciancia M. Salt stress on *Lotus tenuis* triggers cell wall polysaccharide changes affecting their digestibility by ruminants. *Plant Physiol Biochem.* 2021;166:405-415. doi: 10.1016/j.plaphy.2021.05.049